states.—the macroions would immediately deviate from fully stretched conformation. The positive proof for aggregation phenomena inside the macroion domain remains to be obtained, but at the same time there must be required likewise positive proof for the lack of the aggregation almost completely disregarded in previous arguments.

Acknowledgment. We are pleased to extend our thanks to Professor M. Mandel, Leiden, for calling our attention to the water problem in the sample. We are also grateful to Professor T. Higashimura and Dr. M. Sawamoto of our department for their kind help rendered during the Karl-Fischer analysis. Special thanks are due to Dr. Takashi Yamamoto, Tosoh Company Ltd., for his IR, ^{1}H NMR, and ion chromatography analyses of the samples. The generous financial support by the Ministry of Education, Science and Culture is highly appreciated (Grants-in-aid for the Specially Promoted Research, 59065004 and 63060003).

Registry No. NaPSS, 9080-79-9.

Microscopic Observation and Quasielastic Light-Scattering Measurements of Colloid Crystals. Determination of the Radial Distribution Function and Structure Factor for the Two-State Structure

Hiroshi Yoshida, Kensaku Ito, and Norio Ise*

Contribution from the Department of Polymer Chemistry, Kyoto University, Kyoto 606, Japan.
Received May 1, 1989

Abstract: Direct observation by fluorescence microscopy and quasielastic light-scattering (QELS) measurements have been carried out to study particle distributions in polymer latex suspensions. Special attention was paid to the scattering profiles from the two-state structure, in which localized ordered, non-space-filling structures coexisted with disordered regions. From the direct observation, the radial distribution function (RDF) was determined for 35 000 particles by an image data analyzer and further Fourier transformed to the structure factor $S(Q)$. The 2D Fourier analysis (2D FT) of the micrographs was also carried out. The interference function (D_0/D_{eff}), which corresponds to $S(Q)$, was determined by the QELS measurement. The interparticle spacings ($2D_{exp}$) determined from RDF, 2D FT, and QELS measurements were in good agreement and were smaller than those calculated with the assumption of a homogeneous distribution of particles ($2D_0$). Furthermore, $S(Q)$ determined from the direct observation and D_0/D_{eff} determined from the QELS measurement agreed well in both number and position of the peaks. Thus the particle distributions obtained from the microscopic measurements were essentially the same as those obtained by QELS measurements, ruling out the possible vitiating influence of the container wall on the microscopic observation.

I. Introduction

Polymer latex suspensions (particularly polystyrene-based latices) have been intensively studied by microscopic observation and both elastic and quasielastic light-scattering (QELS) measurements.[1-8] By the direct observation technique, the distributions of the particles can be easily photographed,[3,6] although the information derived is on the local, but not global, situation. On the other hand, the scattering techniques are essentially indirect, providing averaged information on the particle distribution. By the direct observation of the suspensions, the coexistence of the ordered structure of a high number density and disordered region having a lower density was confirmed as was shown in Figures 1, 2, and 11 of our previous paper.[9] Such an inhomogeneity in the suspension, which we call the two-state structure, suggests the existence of an (electrostatic) attraction between the particles.[2] Although the ordered structure can be easily distinguished from the disordered region on the bases of the average displacement of the particles, the regularity in the particle distribution, and the number density of the particles, the interference functions determined by the scattering measurements showed only one or two broad peaks. This data has led many authors to the conclusion that there exist no ordered arrangements.

In this report, we determined the particle distribution from the direct observation and concurrently from the QELS measurements for the same sample. The direct observation method is feasible only for relatively large particles, say about 0.2×10^{-6} m in diameter, because of a resolving power of an optical ultramicroscope and of the difference in the refractive indices of the latex and solvent. On the other hand, such large particles cannot be studied by the QELS measurements due to the limitation of Rayleigh-Debye-Gans scattering[10] and the possible disturbance by multiple scattering. Previously,[8] we reported the agreement in the interparticle spacings obtained from the two methods performed independently. To study the same sample by these two methods, a rather small fluorescent latex was used. Although the particles were small (0.14×10^{-6} m in diameter), they could be seen under the fluorescence microscope and micrographs could be taken.

In the present paper, special attention was paid to the two-state structure in the latex suspension. It is attractive to dissect the

(1) Ise, N.; Okubo, T. *Acc. Chem. Res.* **1980**, *13*, 303.
(2) Ise, N. *Angew. Chem., Int. Ed. Engl.* **1986**, *25*, 323.
(3) Kose, A.; Ozaki, M.; Takano, K.; Kobayashi, Y.; Hachisu, S. *J. Colloid Interface Sci.* **1973**, *44*, 330.
(4) Cebula, D. J.; et al. *Faraday Discuss. Chem. Soc.* **1983**, *76*, 37.
(5) Hartl, W.; Versmold, H.; Wittig, U. *Ber. Bunsen-Ges. Phys. Chem.* **1984**, *88*, 1063.
(6) Ise, N.; Okubo, T.; Sugimura, M.; Ito, K.; Nolte, H. J. *J. Chem. Phys.* **1983**, *78*, 536.
(7) Ito, K.; Ise, N. *J. Chem. Phys.* **1987**, *86*, 6502.
(8) Ito, K.; Okumura, H.; Yoshida, H.; Ueno, Y.; Ise, N. *Phys. Rev. B.* **1988**, *38*, 10852.
(9) Ito, K.; Nakamura, H.; Yoshida, H.; Ise, N. *J. Am. Chem. Soc.* **1988**, *110*, 6955.
(10) Kerker, M. *The Scattering of Light and Other Electromagnetic Radiation*; Academic Press: New York, 1969; Chapter 8.

0002-7863/90/1512-592$02.50/0

scattering profiles corresponding to the two-state structure, because only a few groups have claimed such a structure from scattering data of colloid suspensions and macroionic solutions.[11-13] It may be further anticipated that the present analysis that is based on the *real* particle distribution directly observed by microscopy will provide telling information on the structure of liquids in general, which can be studied only by rather indirect methods such as scattering. The radial distribution function (RDF) was newly determined from the particle distributions obtained by the direct observation on fluorescent latex particles forming the two-state structure, and two-dimensional (2D) Fourier analysis was also carried out. By QELS measurements, the interference function was determined and compared with the structure factor $S(Q)$ obtained from the Fourier transformation of the RDF determined by the direct observation.

II. Experimental Section

A. Materials. The fluorescent poly(methyl methacrylate) (PMMA) latex used (MC-6, diameter, 0.14×10^{-6} m; surface charge density, 0.75×10^{-6} C/cm^2) was synthesized with potassium persulfate as an initiator without an emulsifier.[14] As a fluorescent dye, Coumarin 6 (Eastman Kodak Co., Rochester, NY) was used. Because of the presence of the dye, particles could be seen under the fluorescence microscope, even though their diameter was small. The particle charge density was determined by a conductometric titration with analytical-grade 1/100 N NaOH (Wako Junyaku Co., Ltd., Osaka, Japan) using an autobalance precision bridge (Wayne-Kerr Model B331). The titrations were carried out almost at the same time as the microscopic and QELS measurements for the reason discussed previously.[9] The diameter was measured by QELS measurement. The sample was carefully and thoroughly purified by analytical-grade mixed-bed ion-exchange resins AG501-X8(D) (Bio-Rad Laboratories Richmond, CA) and by ultrafiltration method. For details, see ref 9. Completeness of the purification was judged by the appearance of iridescent color in the suspension and the floating phenomena of ion-exchange resin particles.[8,15]

B. Microscopic Observation. The reversed-type fluorescence microscope DIAPHTO TMD with BV fluorescence filter (400–450 nm) was used (Nikon Co., Ltd., Tokyo, Japan). The latex suspensions were filtered through 1.2×10^{-6} m pore-sized disposable filters (Acrodisc, Gelman Science Inc., Ann Arbor, MI) and then introduced to the observation cell (22 mm in diameter), which had a temperature-controlling jacket. The cell was divided into two parts by a horizontal mesh screen, which was 2 mm away from the bottom. The analytical-grade mixed-bed ion-exchange resin (AG501-X8(D)) was introduced to the upper part of the cell for continuous ion exchange. After shaking the sample by an Eyela shaker SS-80 (Tokyo Rikakiki Co., Ltd., Tokyo, Japan) for 6 h at room temperature, the following microscopic observation was started.

The micrographs taken by a video camera C1000 (Hamamatsu Photonics Co., Ltd. Shizuoka, Japan) were image-processed using an image data analyzer SEM-IPS (Carl-Zeiss, Oberkochen, FRG), and the coordinates of the centers of gravity of the particles were determined, as was described previously.[16] By using this information, the RDF's were calculated by the image data analyzer as will be described in Data Analyses. Furthermore, by using the micrograph as a density function, the scattering profiles were calculated by two-dimensional Fourier transformation, as previously described.[7,17]

C. QELS Measurements. The QELS measurements were carried out using a BI2230 with 64 channel correlator (Brookhaven Instruments, Corp., Brookhaven, NY) and the 15-mW He–Ne laser as a light source (Neo-15MS Nihon Kagaku Engineering Tokyo, Japan). The fluorescent dye used (Coumarin 6) had a maximum adsorption at 458 nm, so that the dye could not be excited by the laser used (632.8 nm). As a scattering cell, a carefully washed quartz tube (12 mm in diameter) was used.[8] Suspensions were filtered through disposable filters (Acrodisc, 1.2×10^{-6} m in pore size) before measurements. The analytical-grade mixed-bed ion-exchange resin (AG501-X8(D)) was introduced into the cell to remove further ionic impurities. The autocorrelation functions were analyzed by the cumulant method[18] and the interference functions (D_0/D_{eff}) were determined as previously reported.[8,18]

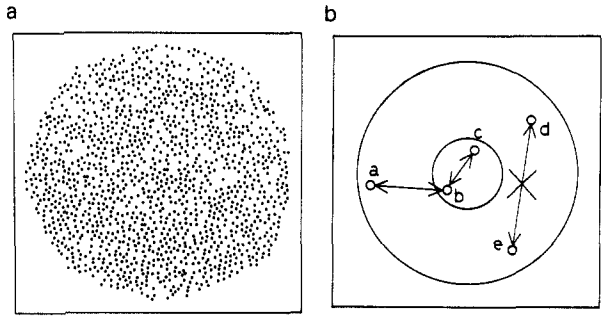

Figure 1. Computer-treated particle distribution in binary image (a) and scheme for calculation of the radial distribution function (b). In (b), the diameter of the inner circle is $^1/_3$ of the diameter of the outer circle showing the region where particles exist.

D. Data Analyses. The RDF is usually determined by scattering techniques.[19] From QELS measurements, however, it is experimentally difficult to obtain the interference function in the small scattering vector region, which is important to determine the RDF. Thus, we determined the RDF from a direct observation method, namely by measuring interparticle distances on the micrographs. The influence of the limited area of the field of view on the RDF was eliminated by the method described in Figure 1. Figure 1a shows an example of the particle distribution obtained by the microscopic observation and image processing. In Figure 1b, the region where particles exist is shown by the outer circle. The inner circle has a diameter that is $^1/_3$ that of the outer circle. For the particles inside the inner circle, all surrounding particles whose interparticle distances are smaller than the diameter of the inner circle exist inside the outer circle: This means that no "*termination* effect" is involved so far as the particles inside the inner circle are concerned. Thus by measuring the interparticle distances only from the particles inside the inner circle (like the distance between particles a and b or b and c), the influences caused by the limited measurement area on RDF were eliminated, so far as distances smaller than the diameter of the inner circle are concerned. The particle distribution image that can be obtained by microscopy is a projection onto a horizontal plane of particles existing in the focal volume, which is the product of the depth of focus and the area of visual field. Thus, as will be described below, the RDF determined ($f(x,y)$) is the integration of the real three-dimensional RDF ($g^3(x,y,z)$) from $-d/2$ to $d/2$, where d is the thickness of the focal volume (=depth of focus).

$$f(x,y) = \int_{-d/2}^{d/2} g^3(x,y,z)\, dz$$

However, if d is sufficiently small and the particle distribution is isotropic, $f(x,y)$ becomes equal to the product of $g^3(x,y,z)$ and d. Thus

$$\lim_{d\to 0} f(x,y) = \lim_{d\to 0} \int_{-d/2}^{d/2} g^3(x,y,z)\, dz = d\, g^3(x,y,0)$$

By dividing $f(x,y)$ by d, the three-dimensional RDF was calculated. The d can be expressed as follows

$$d = n\frac{\epsilon}{m\mathrm{NA}}$$

where n is the refractive index of the immersion oil, ϵ is the diameter of the circle of least confusion, m is the total magnification, and NA is the numerical aperture. To check whether d is sufficiently small or not, we examined the RDF by changing the total magnification, m, from 375 to 990 (0.11×10^{-6} to 0.04×10^{-6} m in d); we observed little change in RDF's. Therefore, d was sufficiently small. The d used in practice was 0.11×10^{-6} m ($n = 1.47$, $\epsilon = 0.036$ mm, $m = 375$, and NA = 1.3) and altogether about 35000 particles were treated to obtain the RDF.

To compare the results derived from the direct observation and the QELS measurements, the RDF determined by the former was Fourier-transformed to the structure factor $S(Q)$ numerically as follows

$$S(Q) = \frac{N}{V}\int \{g(r) - 1\} \exp(i\mathbf{Q}\cdot\mathbf{r})\, d\mathbf{r} = \frac{N}{V}\int \{g(r) - 1\}\frac{\sin(Qr)}{Qr} 4\pi r^2\, dr$$

(11) Ise, N.; et al. *J. Am. Chem. Soc.* **1980**, *102*, 7901.
(12) Clark, N. A.; Ackerson, B. J.; Hurd, A. J. *Phys. Rev. Lett.* **1983**, *19*, 1459.
(13) Yoshiyama, T.; Sogami, I.; Ise, N. *Phys. Rev. Lett.* **1984**, *22*, 2153.
(14) Ono, H.; Saeki, H. *Colloid Polym. Sci.* **1975**, *253*, 744.
(15) Ise, N.; Okubo, T.; Kitano, H.; Sugimura, M.; Date, S. *Naturwissenschaften* **1982**, *69*, 544.
(16) Ito, K.; Nakamura, H.; Ise, N. *J. Chem. Phys.* **1986**, *85*, 108.
(17) Murry, C. A.; van Winkle, D. H. Private Communication.
(18) Pusey, P. N.; Thogh, R. J. A. *Dynamic Light Scattering*; Pecora, R., Ed.; Plenum: New York, 1985; Chapter 4.
(19) Guinier, A.; Fournet, G. *Small-Angle Scattering of X-Rays*; John Wiley & Sons, Inc.: New York, 1955; Chapter 2.

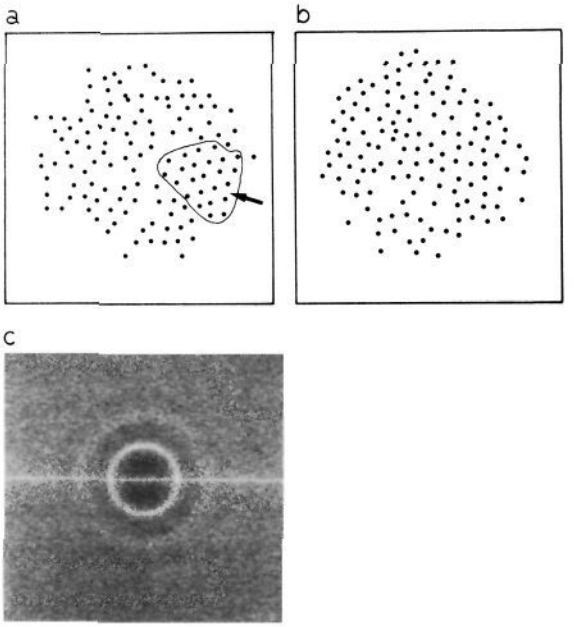

Figure 2. Computer-treated binary images of the two-state structure of MC-6 latex suspension (a,b) and the corresponding Fourier pattern (c). Since it is almost impossible to distinguish the particles in the ordered structure from those in coexisting disordered regions on still pictures like the present one, the ordered particles in (a) are conveniently surrounded by a closed curve and pointed to by an arrow. In reality, the motion of the ordered particles is discernible from that of the free particles. See Figure 11 of ref 9. Latex conc, 0.15 vol %; diameter, 0.14×10^{-6} m; temp, 25 °C.

where Q is the scattering vector, r is the distance, and N/V is the number of particles in the unit volume. In Fourier transformation of $g(r)$ a damping factor df was used,[20] which is expressed as

$$\mathrm{df} = \exp(-ar^2)$$

where a is a constant.

III. Results and Discussion

Fluorescence Micrographs, Their Fourier Patterns, Radial Distribution Functions, and Interparticle Spacings. Parts a and b of Figure 2 show the distribution of the centers of gravity of particles for MC-6 observed by the fluorescence microscope at a concentration of 0.15% at 25 °C. To obtain micrographs of a sharp contrast, the iris had to be very small. Thus, a very limited number of particles could be pictured. Accordingly, the 2D Fourier transformation had to be carried out by using three composite pictures, each being composed of 16 distribution images such as shown in parts a and b of Figure 2. The transformation was performed by the method described previously,[7] and Figure 2c shows the Fourier pattern obtained. A clear first-order peak and the second halo, though not clear, are seen. By assuming the face-centered-cubic (fcc) symmetry, the closest interparticle distance $2D_{exp}$ was obtained.

The RDF was calculated by using about 300 distribution images involving about 35 000 particles (Figure 3). From the first peak, the interparticle distance $2D_{exp}$ was determined.

Figure 4 shows the D_0/D_{eff} (open circles) determined by the QELS method for the same sample, MC-6. Clearly two peaks, though broad, are seen, which appear to correspond to the Fourier patterns derived above. Again by assuming a fcc symmetry, the interparticle distance $2D_{exp}$ was estimated from the first peak.

Three values of $2D_{exp}$ thus obtained from 2D FT, RDF, and QELS are listed in Table I. The three values were in good agreement with each other. Furthermore, the $2D_{exp}$ value was smaller than $2D_0$, the average interparticle distance, which can be estimated from the particle concentration by assuming a uniform distribution of the particles throughout the suspension. This tendency has been observed for high charge density latex particles by microscopy and for high charge density ionic polymers by scattering technique and is now further reinforced by the present experiments. As is clear from Table I, the $2D_{exp}$ was practically independent of temperature, whichever of the three methods was used for its determination. This confirms our previous finding that the spacing is not sensitive to temperature.[21] As was discussed recently,[22] such a tendency is quite acceptable since the ordered structure expands as the temperature rises, causing larger spacing, and simultaneously the dielectric constant

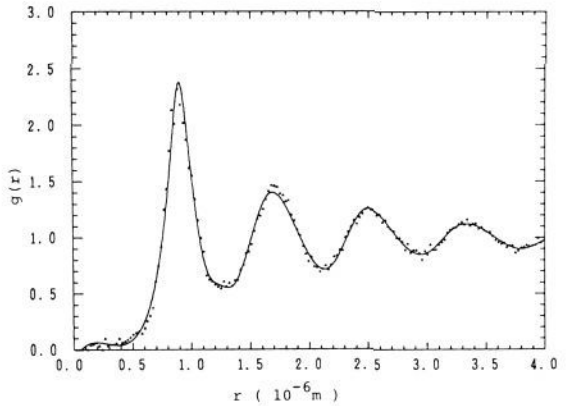

Figure 3. Radial distribution function $g(r)$ of the MC-6 latex suspension forming the two-state structure determined by the direct observation method. Latex conc, 0.15 vol %; diameter, 0.14×10^{-6} m; temp, 25 °C.

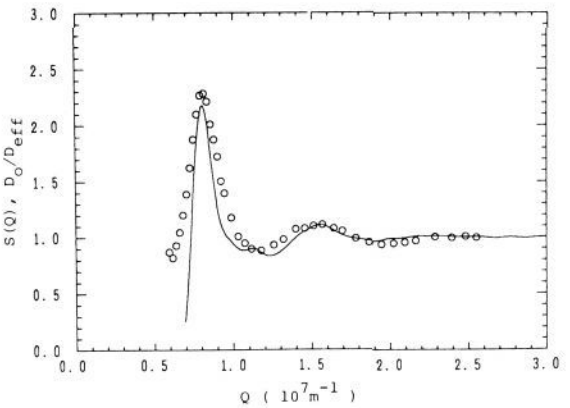

Figure 4. Interference function D_0/D_{eff} determined by the QELS measurement and structure factor $S(Q)$ determined by the Fourier transformation of $g(r)$ versus scattering vector Q: ○, D_0/D_{eff}; solid line, $S(Q)$; latex, MC-6; latex conc, 0.15 vol %; diameter, 0.14×10^{-6} m; temp, 25 °C.

Table I. $2D_{exp}$'s Determined from RDF, 2D FT, and QELS Measurements[a]

concn, vol %	temp, °C	$2D_{exp}$, 10^{-6} m			$2D_0$, 10^{-6} m
		RDF	2D FT	QELS	
0.15	20	0.91	0.95	0.97	1.11
	25	0.89	0.95	0.95	
	30	0.89	0.92	0.90	
	50	0.88	0.95	0.98	
0.10	20	0.98	1.02	1.05	1.27

[a] latex, MC-6; diameter, 0.14×10^{-6} m; surface charge density, 0.75×10^{-6} C/cm^2.

(20) Klug, H. P.; Alexander, L. E. *X-Ray Diffraction Procedures*; John Wiley & Sons, Inc.: New York, 1974; p 823.

(21) Ise, N.; Ito, K.; Okubo, T.; Dosho, S.; Sogami, I. *J. Am. Chem. Soc.* **1985**, *107*, 8074.

(22) Ise, N.; Matsuoka, H.; Ito, K.; Yoshida, H.; Yamanaka, J. *Langmuir*, in press.

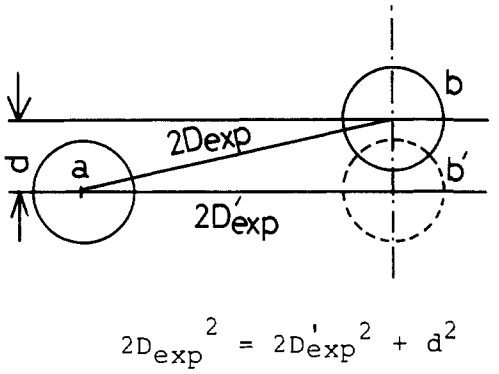

Figure 5. Influence of the depth of the focal volume d on the $2D_{exp}$ measured by the direct observation.

of water is lowered so that electrostatic interparticle *attraction* is enhanced, causing smaller spacing: when these two counteracting influences cancel out, $2D_{exp}$ would stay unchanged as was shown in Table I.

In this respect, we note that the spacing must become larger (instead of staying constant as was observed experimentally), if the generally accepted "repulsion-only" assumption is right, since both the thermal energy contribution and the repulsion must then be enhanced by the temperature rise. The experimental finding is opposite: the spacing did not increase with the temperature rise.

It should be further emphasized that the degree of dissociation of latex particles has been established to be insensitive toward temperature according to the conductance measurements.[22] This implies that, when we discuss the observed temperature insensitivity of $2D_{exp}$, the change of the degree of dissociation of latex particles with temperature, and hence the actual (not analytical) valency, need not be taken into consideration. Thus, the changes of dielectric constant and thermal motion with temperature may be understood to influence the interparticle distance in a more direct manner (not through variation of the valency).

Depth of Focus. The next factor to be considered is the depth of focus of the microscopy. As is shown in Figure 5, if the depth (d) is large, the (real) interparticle distance ($2D_{exp}$) could be underestimated: the particle at b would be observed as if it is located at b', so that the observed interparticle distance is shorter than the real one. As was often pointed out, we observed $2D_{exp} < 2D_0$ (average interparticle distance) for high charge density solutes. It may be questioned whether this shortening for latex cases is an artifact due to the optical illusion. However, the value of d is small enough in our system. By using the actual d value (0.11×10^{-6} m) and a $2D_{exp}'$ value (0.9×10^{-6} m), the difference between $2D_{exp}$ and $2D_{exp}'$ was found to be only 0.007×10^{-6} m, which is within the experimental error.

Structure Factors from Radial Distribution Function and Quasielastic Light Scattering. In Figure 4 are compared the structure factors from the RDF (curve) and from the QELS (open circles). As far as the peak position and the number of peaks are concerned, the two methods provide consistent results.[23] This fact implies that, even when broad scattering peaks as shown in Figure 4 have been observed, we must admit the existence of an ordered structure or at least the coexistence of (non-space-filling) ordered structures and disordered regions in the two-state structure. This consequence is in line with an independent theoretical calculation of the structure factor based on paracrystal lattices by Matsuoka et al.[24] According to the theory, the height and number of the peaks of the structure factor become smaller with increasing degree of paracrystal distortion and Debye–Waller effect, and with decreasing crystal size. Therefore, the results described in the present paper and the theoretical consideration corroborate that *the observation of one or two broad scattering peaks proves some kind of structuredness (though distorted) of solute species in solutions or suspensions*, although the opposite has been claimed widely.

IV. Concluding Remarks

In the present paper, the microscopic investigation and the QELS measurement were concurrently carried out on *one* latex sample. The RDF of the latex distribution was directly determined from the micrographs showing the two-state structure and Fourier transformed into the structure factor $S(Q)$. The $S(Q)$ was independently determined from the QELS measurements. Also the scattering profile was obtained by the 2D Fourier transformation of the micrographs (as density functions). The interparticle distance ($2D_{exp}$) was estimated from the three methods, namely the RDF, 2D FT, and QELS. The values obtained by the three methods agreed well with each other. The $2D_{exp}$ thus found was smaller than the average distance ($2D_0$) derived from latex concentration, confirming our previous results.[1,2] Furthermore, the $2D_{exp}$ hardly changed with temperature in the range studied (20–50 °C), again supporting our previous data.[21]

A comment seems to be necessary on the agreement between the microscopic and QELS observation. As was repeatedly mentioned, the microscopic method provides information in the local area not far from the cover glass (container wall). On the other hand, the QELS measurements furnish averaged information on the solute distribution inside solution or suspension (far away from the container wall). Thus, the agreement we obtained between the two methods indicates that, in the microscopic investigation, *the wall effect is not so serious, if at all, as far as the solute distribution (particularly the interparticle distance) is concerned.*[25]

It seems, thus, quite legitimate to claim that the present work firmly warrants the reliability of our microscopic study. Thus, we would be able to claim that the inequality relation, $2D_{exp} < 2D_0$, holds not only in the area close to the cover glass but also inside the suspensions. Taking into consideration the fact that the inequality relation not only has also been observed for latex suspensions but also has been confirmed by X-ray and neutron scattering techniques for soluble macroions, the relation is certainly an important one, which reflects the very nature of the intermacroion and interparticle interactions. This corroborates our previous assertion that there exists an electrostatic attraction between particles or macroions through the intermediary of counterions. Experimental evidence supporting the existence of the attraction has been discussed.[2,22] Among various experimental facts, the recent observation[27] that the Ostwald ripening mechanism is valid in the process of crystallization of latex particles appears most positively to testify to the attraction.

Acknowledgment. We express our sincere thanks to Professor Hiromi Yamakawa for his advice and discussion during this work,

(23) For the Fourier transformation of the RDF to the structure factor $S(Q)$, 8.0×10^6 cm^{-2} was used for the a in the damping factor.

(24) Matsuoka, H.; Tanaka, H.; Hashimoto, T.; Ise, N. *Phys. Rev. B* **1987**, *36*, 1754; corrections in press.

(25) There remains a problem to be considered carefully. As was described before,[26] the (111) plane of a fcc symmetry or the (110) plane of a bcc structure is often observed by microscopy. One interesting phenomenon is that this happens not only on a horizontal cover glass but also along a vertical cover glass. If the close-packed plane *were* observed only on a horizontal plane, a sedimentation effect by the gravity must be taken seriously as a cause. However, the fact that the close-packed plane can be found also along the vertical plane appears to rule out the sedimentation effect. Instead, some kind of affinity between the particles and the cover glass, horizontal or vertical, would have to be admitted. This affinity would force the particles to come to the vicinity of the glass surface and to form an ordered structure with the possible maximum packing efficiency along the glass surface. Once the first layer is formed, the particles of that layer would attract other particles (through the intermediary of counterions) to form the second layer, which further induce the third layer and so on. Thus a three-dimensional ordered structure would be completed. When the particle concentration is rather low and the kinetic energy contribution is high, the ordered structure would be partially destroyed: then, localized ordering might be observed. Unfortunately, we do not know anything about the nature of the affinity between the glass surface and the latex particles at present: a systematic study is in progress by using chemically modified glass surfaces.

(26) Ito, K.; Nakamura, H.; Ise, N. *J. Chem. Phys.* **1986**, *85*, 6136.

(27) Ito, K.; Okumura, H.; Yoshida, H.; Ise, N. *J. Am. Chem. Soc.* **1989**, *111*, 2347.

particularly on the transformation of the two-dimensional information to the three-dimensional distribution function. We express our sincere thanks to Professors Norio Nemoto and Takeji Hashimoto for their advice on the QELS experiments. This work was made possible by generous support from the Ministry of Education, Science and Culture (Grants-in-Aid for specially promoted research 59065004 and 63060003) and the Japan Society for the Promotion of Science (K.I.).

Registry No. PMMA, 9011-14-7.

Insertion and σ-Bond Metathesis Pathways in Gas-Phase Reactions of Bis(η^5-cyclopentadienyl)methylzirconium(1+) with Dihydrogen and Unsaturated Hydrocarbons

Charles S. Christ, Jr., John R. Eyler, and David E. Richardson*,†

Contribution from the Department of Chemistry, University of Florida, Gainesville, Florida 32611. *Received March 13, 1989*

Abstract: Reactions of $Cp_2ZrCH_3^+$ (**1**: Cp = cyclopentadienyl) and $Cp_2ZrCD_3^+$ (**2**) with a number of unsaturated hydrocarbon substrates and dihydrogen have been investigated. Reactions of **2** with hydrocarbon substrates and C_2D_4 with **1** support two major reaction pathways: insertion/dehydrogenation, which is accompanied by near statistical H/D scrambling, and σ-bond metathesis, which is indicated by the exclusive elimination of CD_3H in reactions of **2** with certain substrates. Reactions of **1** and **2** with ethylene and α-alkyl-substituted alkenes result in elimination of dihydrogen and formation of η^3-allyl complex cations. For reaction of **1** and **2** with α-alkyl-substituted ethylenes having *n*-alkyl substituents larger than ethyl (e.g., 1-pentene, 1-hexene) elimination of H_2 and $2H_2$ occurs, and in the current study products formed with H_2 elimination are always found in greater abundance. Reactions of **2** with α,α'-substituted alkenes (e.g., isobutene and α-methylstyrene) proceed with elimination of CD_3H exclusively, which is consistent with a σ-bond metathesis process. Reaction of **2** with isobutene also yields **1**, suggesting an insertion/β-methide shift/isobutene elimination sequence. Cation **1** is also produced in the reaction of **2** with propyne. Reaction of Cp_2ZrD^+ with ethylene shows formation of Cp_2ZrH^+, suggesting an insertion/β-hydride shift/ethylene elimination process, presumably because a η^3-allyl product cannot be formed by elimination of H_2. Reactions of **1** and **2** with cis and trans isomers of 2-butene and 2-pentene have also been investigated, and striking reactivity differences are observed for the two isomers (i.e., cis isomers react predominantly by an insertion/dehydrogenation pathway and trans isomers react almost exclusively by elimination of methane). Products consistent with both insertion/dehydrogenation and σ-bond metathesis are suggested by results of reactions of **1** and **2** with several alkynes. The reaction of **2** with H_2 proceeds with exclusive elimination of CD_3H, also indicating a σ-bond metathesis process. Rate constants for the reaction of **1** with H_2 and D_2 yield a k_H/k_D value of 2.0 ± 0.5. The reactivity of **1** with unsaturated hydrocarbons is compared to the solution reactions of the analogous solvated cation and other d^0f^n metal complexes.

Despite explosive growth in the field of organometallic chemistry of solvated complexes and gas-phase metal ions, few studies directly comparing the reactivity of organometallic compounds in the gas-phase and solution have appeared. Such gas-phase/solution comparisons have provided significant insight into the chemistry of organic compounds[1-6] in reactions such as group transfer and proton transfer. We have previously reported direct comparisons of this type for electron-transfer reactions of the metallocenes,[7a] displacement reactions involving anionic organometallic nucleophiles,[7b] and reactions of highly electrophilic d^0 complexes with dihydrogen, ethylene, and propylene.[7c] We report here further investigations of the gas-phase reactions of electrophilic zirconium(IV) complexes with unsaturated hydrocarbons. These initial gas-phase studies show many similarities to reactivity observed for lanthanide, actinide, and early-transition-metal complexes in solution, and, furthermore, new reaction pathways are observed that may eventually be found for related complexes in solution.

High reactivity and potential usefulness have led to considerable interest in the reactions of electrophilic organometallic complexes in solution.[8-13] Condensed-phase reactions of neutral and cationic d^0 and d^0f^n metal alkyls and hydrides with organic substrates have been studied extensively.[14-16] Several examples of electrophilic ethylene polymerization catalysts have been discovered, and many of these complexes undergo transformations closely related to fundamental processes proposed for Ziegler-Natta catalysts

† A. P. Sloan Foundation Research Fellow, 1988-1990.

(1) (a) Stevenson, G. R.; Reiter, R. C.; Espe, M. E.; Bartmess, J. E. *J. Am. Chem. Soc.* **1987**, *109*, 3847. (b) Rozeboom, M. D.; Kiplinger, J. P.; Bartmess, J. E. *J. Am. Chem. Soc.* **1984**, *106*, 1025.
(2) Dillow, G. W.; Kebarle, P. *J. Am. Chem. Soc.* **1988**, *110*, 4877.
(3) Dodd, J. A.; Brauman, J. I. *J. Phys. Chem.* **1986**, *90*, 3559.
(4) Bohme, D. K.; Raksit, A. B. *Can. J. Chem.* **1985**, *63*, 3007.
(5) (a) Meot-Ner, M. *J. Am. Chem. Soc.* **1987**, *109*, 7947. (b) Nelson, S. F.; Rumack, D. T.; Meot-Ner, M. *J. Am. Chem. Soc.* **1988**, *110*, 3071.
(6) Caldwell, G.; McMahon, T. B.; Kebarle, P.; Bartmess, J. E.; Kiplinger, J. P. *J. Am. Chem. Soc.* **1985**, *107*, 80.
(7) (a) Richardson, D. E.; Christ, C. S.; Sharpe, P.; Eyler, J. R. *J. Am. Chem. Soc.* **1987**, *109*, 3894. (b) Richardson, D. E.; Christ, C. S.; Sharpe, P.; Eyler, J. R. *Organometallics* **1987**, *6*, 1819. (c) Christ, C. S.; Eyler, J. R.; Richardson, D. E. *J. Am. Chem. Soc.* **1988**, *110*, 4038.
(8) Green, M. L. H. *Pure Appl. Chem.* **1985**, *57*, 1897.
(9) Parshall, G. W. *CHEMTECH* **1984**, *14*, 628.
(10) Evans, W. J. *Adv. Organomet. Chem.* **1985**, *24*, 131.
(11) Crabtree, R. H. *Chem. Rev.* **1985**, *85*, 245.
(12) Watson, P. L. *Acc. Chem. Res.* **1985**, *18*, 51.
(13) den Haan, K. H.; Wielstra, Y.; Meetsma, A.; Teuben, J. H. *Organometallics* **1987**, *6*, 2053.
(14) (a) Jordan, R. F. *J. Chem. Educ.* **1988**, *65*, 285. (b) Jordan, R. F.; Lapointe, R. E.; Bajgur, C. S.; Echols, S. F.; Willett, C. S. *J. Am. Chem. Soc.* **1987**, *109*, 4111. (c) Jordan, R. F.; Bajgur, C. S.; Dasher, W. E. *Organometallics* **1987**, *6*, 1041.
(15) (a) Thompson, M. E.; Bercaw, J. E. *Pure Appl. Chem.* **1984**, *56*, 1. (b) Thompson, M. E.; Bercaw, J. E. *J. Am. Chem. Soc.* **1987**, *109*, 203. (c) Doherty, N. M.; Bercaw, J. E. *J. Am. Chem. Soc.* **1985**, *107*, 2670.

0002-7863/90/1512-596$02.50/0